

Setting Risk-Informed Environmental Standards for *Bacillus Anthracis* Spores

Tao Hong,¹ Patrick L. Gurian,^{1,*} and Nicholas F. Dudley Ward²

In many cases, human health risk from biological agents is associated with aerosol exposures. Because air concentrations decline rapidly after a release, it may be necessary to use concentrations found in other environmental media to infer future or past aerosol exposures. This article presents an approach for linking environmental concentrations of *Bacillus anthracis* (*B. anthracis*) spores on walls, floors, ventilation system filters, and in human nasal passages with human health risk from exposure to *B. anthracis* spores. This approach is then used to calculate example values of risk-informed concentration standards for both retrospective risk mitigation (e.g., prophylactic antibiotics) and prospective risk mitigation (e.g., environmental clean up and reoccupancy). A large number of assumptions are required to calculate these values, and the resulting values have large uncertainties associated with them. The values calculated here suggest that documenting compliance with risks in the range of 10^{-4} to 10^{-6} would be challenging for small diameter (respirable) spore particles. For less stringent risk targets and for releases of larger diameter particles (which are less respirable and hence less hazardous), environmental sampling would be more promising.

KEY WORDS: Bioterrorism; environmental standards; microbial risk assessment

1. INTRODUCTION

The 2001 anthrax attacks precipitated an aggressive response in which large numbers of potentially exposed people were treated with prophylactic antibiotics, and contaminated buildings were remediated until no detectable *B. anthracis* spores were present.^(1,2) These actions appear to have been effective in saving lives, but the response was expensive, raising the question as to how standards may be set that prioritize response actions based on risk. The use of risk-informed standards has become part of the statutory drinking water standard setting process in the United States,⁽³⁾ and risk estimates are re-

quired for all major regulations in the United States as part of the benefit-cost analysis requirements of Executive Order 12291.⁽⁴⁾ The risk-based approach can be justified on the grounds that it allows for risk-risk tradeoffs in decision making (e.g., one can balance the risk of anthrax against the risks of side effects from prophylactic medical treatment) and can allow for risk reduction efforts to be directed toward the greatest risks.

While valuable contributions have been made toward understanding a wide range of response issues related to *B. anthracis*, including environmental transport,^(5–8) dose response,^(9–13) impacts of a release,^(14–19) and effectiveness of environmental sampling,^(20–28) at the present there are still no quantitative environmental standards for *B. anthracis*. Negative sampling results are generally taken as evidence that a building is not contaminated with *B. anthracis*, but a negative sample does not establish zero risk, as sampling variability can lead to a negative result.⁽²⁸⁾

¹ Department of Civil, Architectural and Environmental Engineering, Drexel University, Philadelphia, PA, USA.

² Pattle Delamore Partners, New Zealand.

*Address correspondence to Patrick Gurian, Alumni Engineering Labs, Rm. 270-K, 3141 Chestnut St., Philadelphia, PA 19104, USA; tel: 1-215-895-2885; fax: 1-215-895-1363; pgurian@drexel.edu.

This article proposes an approach to developing environmental standards for *B. anthracis*, and identifies sampling requirements, which, if negative results are obtained, would provide a degree of confidence that these standards had been met. Available literature information is then used to calculate example values for environmental standards and sampling requirements. While the values presented here are not intended to be suitable for adoption by regulatory agencies, the effort is intended to inform future work in this area. In particular, the development of the standards relies on a large number of assumptions. This effort seeks to clearly identify these assumptions and where feasible to employ health-protective assumptions in calculating standards. Future work could be aimed at replacing these health-protective assumptions with more realistic models, which could lead to less stringent standards.

This article begins with a qualitative discussion of the approach proposed here, and then develops an integrated mathematical model of the environmental transport, exposure, and health risk following a release of *B. anthracis* spores. This model is used to link environmental concentrations of *B. anthracis* to health risk, so that once a particular target level of health risk is specified, then environmental concentration standards corresponding to this risk level can be computed. The model is applied to a simplified case, a hypothetical building consisting of a single small room, and example concentration standards are calculated.

2. ASSUMPTIONS FOR STANDARDS

Standards are meant to inform decisions and in the case of a release of a pathogenic microorganism, decision making differs based on whether one is concerned with the risk to which occupants of a space were exposed in the past (termed retrospective risk here) or the risk to which occupants will be exposed in the future (termed prospective risk here). Retrospective risk estimates would inform measures for mitigating prior exposures, such as administering prophylactic antibiotics, while prospective risk estimates would inform decisions for mitigating future exposures, such as environmental remediation and reoccupancy standards for contaminated buildings. Thus, this analysis develops two sets of standard setting processes, one for retrospective risk and one for prospective risk.

This analysis addresses inhalation risk only. This pathway was selected for initial consideration because of the high risk of fatality via the inhalation

pathway; 89–96% for untreated cases, 45% among the 2001 anthrax attack cases who received treatment. In contrast, dermal anthrax has a lower fatality risk of 5–20%.^(29,30) However, much of the risk in the prospective case may be due to dermal exposure, as spores may tend to bind irreversibly to surfaces over long periods of time, making reaerosolization difficult.⁽³¹⁾ Thus extending this effort to address dermal risk is a priority for future efforts.

This analysis assumes uniform mixing of the released *B. anthracis* spores throughout the air of a room. This assumption can miss localized areas of high risk, such as a highly concentrated puff of spores generated by opening a contaminated letter. This assumption is more appropriate for conditions somewhat removed in time and space from the initial release, such as rooms or even buildings located downgradient from the initial release. It is precisely in these downgradient areas that difficult decisions about prophylactic treatment of occupants and remediation will need to be made since both treatment and remediation will almost certainly be required in the immediate vicinity of the release. If this approach is to be applied in the room in which a release took place, then it would be applicable only to exposures that occur after some internal mixing has occurred.

Both deposition rates and dose response vary greatly with particulate size. Therefore, in this analysis separate standards are developed for four different aerodynamic diameters: 1, 3, 5, and 10 μM . These values span the range from the diameter of a single spore (roughly 1 μM) to the point at which deposition rates would dominate over mixing processes (diameters $> 10 \mu\text{M}$) and an analysis such as this, based on uniform mixing, would no longer be appropriate. This is another reason why this approach is most appropriately applied to areas removed from the initial release, as larger particles ($\geq 10 \mu\text{M}$) may be present in substantial numbers in the immediate vicinity of a release. Condensation reactions (particle aggregation) are not considered here as these processes are not important for more dilute mixtures. Because smaller size fractions present the greatest inhalation risk, both the assumption that the *B. anthracis* spores are present as fine particulates and that these particulates do not aggregate, are health protective.

The dose-response models used in this approach are based on studies in which animals were exposed to a single, large (i.e., bolus) dose of organisms. Such large doses may overwhelm natural immune responses and overestimate risks due to lower exposures. Thus, the use of risks associated with a

single high dose is a health-protective assumption. However, humans may be more or less sensitive to pathogens than other animals. To address this, a range of values for dose response are based on a meta-analysis⁽³³⁾ of experiments involving a number of different species and the upper end of this range is intended to be reflective of more sensitive species.

This analysis does not consider decay over time. This assumption is health protective and in accordance with studies that have shown that *B. anthracis* spores can persist for decades in protected environments.^(34,35) This analysis also assumes that an individual is continuously present in the room where risk is to be quantified. This is health protective as it maximizes the human exposure associated with a given release. An additional health-protective assumption is that all organisms quantified by sampling are considered to be viable.

3. METHODS

3.1. Integrated Modeling Approach

The environmental transport model considers a simple office with a heating ventilation and air conditioning (HVAC) system as in Fig. 1. The office is divided into eight internal compartments: air, tracked floor (horizontal surfaces from which spores may be resuspended by walking or other activities), untracked floor (horizontal surfaces from which there is no resuspension), walls, HVAC, all areas external

The air and tracked floor can exchange spores with each other but the remaining six compartments (walls, untracked floor, ceiling, HVAC filter, nasal passages, and external compartment) accumulate spores irreversibly from the air compartment. As a result, concentrations in the tracked floor and air compartments will asymptotically approach zero, and concentration in the remaining compartments will asymptotically approach constants.

The numbers of spores in the compartments are denoted by M_{air} (air), M_{tf} (tracked floor), M_{utf} (untracked floor), M_w (walls), M_f (filter), M_{ec} (external compartment), M_{ce} (ceiling), and M_n (nasal passages). Deposition from the air compartment is modeled as a first-order process with rate constants (units of s^{-1}) of λ_{tf} (deposition to tracked floor), λ_{utf} (untracked floor), λ_w (walls), and λ_{ce} (ceiling). A second source of removal is by the HVAC system. The total air flow rate through the HVAC system is denoted by Q (units of m^3/s), p (dimensionless) is the fraction of total air flow that is recirculated into the building by the HVAC system, e (dimensionless) is the efficiency of the filter at removing particles, and V is the volume of the room (m^3). Removal to the occupants' nasal passages is also modeled with I (m^3/s), denoting the breathing flow rate, and e_n (dimensionless), the efficiency of the nasal passages at removing particles. Resuspension from the tracked floor due to occupants walking and other activities is also modeled as a first-order process with rate constant μ_2 (units of s^{-1}). This model is described mathematically by the following system of ordinary linear first-order differential equations:

$$\frac{dM}{dt} = \begin{pmatrix} \dot{M}_{air} \\ \dot{M}_{tf} \\ \dot{M}_{utf} \\ \dot{M}_w \\ \dot{M}_f \\ \dot{M}_{ec} \\ \dot{M}_{ce} \\ \dot{M}_n \end{pmatrix} = \begin{pmatrix} [(1-e)p-1]\frac{Q}{V} - (\lambda_{tf} + \lambda_{utf} + \lambda_w + \lambda_{ce} + Ie_n) & \mu_2 & 0 & 0 & 0 & 0 & 0 & 0 \\ \lambda_{tf} & -\mu_2 & 0 & 0 & 0 & 0 & 0 & 0 \\ \lambda_{utf} & 0 & 0 & 0 & 0 & 0 & 0 & 0 \\ \lambda_w & 0 & 0 & 0 & 0 & 0 & 0 & 0 \\ ep\frac{Q}{V} & 0 & 0 & 0 & 0 & 0 & 0 & 0 \\ (1-p)\frac{Q}{V} & 0 & 0 & 0 & 0 & 0 & 0 & 0 \\ \lambda_{ce} & 0 & 0 & 0 & 0 & 0 & 0 & 0 \\ \frac{Ie_n}{V} & 0 & 0 & 0 & 0 & 0 & 0 & 0 \end{pmatrix} \begin{pmatrix} M_{air} \\ M_{tf} \\ M_{utf} \\ M_w \\ M_f \\ M_{ec} \\ M_{ce} \\ M_n \end{pmatrix} \quad (1)$$

to the room, ceiling, and the nasal passages of an occupant of the office.

Once initial conditions are specified, this system can be solved using standard approaches, which are described in the Appendix. Different initial

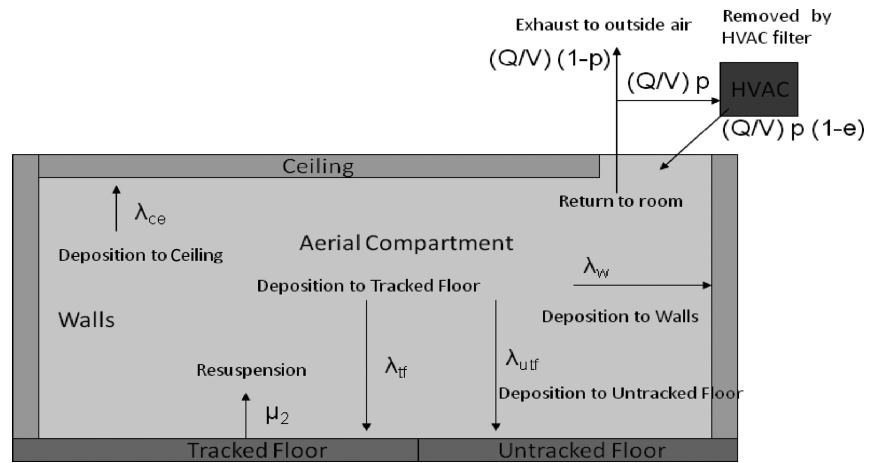


Fig. 1. Schematic of model.

conditions are used for the retrospective and prospective scenario. In the retrospective scenario, all spores are initially present in the air compartment and surface concentrations at the end of the scenario are linked to risk (i.e., one wishes to assess the risks posed by a release in the air compartment based on what surface samples indicate the past exposures were). In the prospective case, all spores are initially present on the tracked floor and surface concentrations at the start of the scenario are linked to risk (i.e., the initial aerosol release has dissipated and one wishes to assess the risks associated with deposited spores that may be reaerosolized in the future).

Once the mass and concentrations in each compartment are computed, the inhaled dose of *B. anthracis* is calculated by integrating the inhalation rate and concentration of *B. anthracis* in the air, over the duration of the exposure:

$$dose = I \int_{t_1}^{t_2} C_{air}(t) dt, \tag{2}$$

where I is the human breathing rate with the unit m^3/s ; $C_{air}(t)$ is the concentration of *B. anthracis* in the air compartment with the unit spores/ m^3 ; and $t_2 - t_1$ is the exposure interval for occupants in that room.

Previous studies indicate that the exponential dose-response model⁽³⁶⁾ (Equation (3)) provides a favorable fit for *B. anthracis* spores with particle size smaller than $5 \mu M$, and the beta-Poisson function⁽³⁶⁻⁴⁰⁾ (Equation (4)) fits well for spores with diameters larger than $5 \mu M$:^(11,12)

$$risk = 1 - \exp(-r \text{ dose}), \tag{3}$$

$$risk \approx 1 - \left(1 + \frac{\text{dose}}{\beta}\right)^{-\alpha}, \tag{4}$$

where risk is the probability of mortality, dose is the average number of inhaled spores, r is the probability that a single organism will survive to initiate infection, and α, β are parameters of a beta distribution describing variability in survival probability. When the product of r and dose is relatively small, a first-order Taylor series can be used to approximate Equations (3) and (4) as:

$$risk \approx r \text{ dose}, \tag{5}$$

$$risk \approx \frac{\alpha}{\beta} \text{dose} = \frac{\alpha}{\left(\frac{N_{50}}{2^{1/\alpha} - 1}\right)} \text{dose}, \tag{6}$$

where N_{50} is median lethal dose. Since the initial conditions for retrospective and prospective risk are different, we consider these two different scenarios separately in the following.

3.2. Retrospective Risk

Concentrations in several of the environmental compartments are linear functions of the integral of past air concentrations. As the dose is also a function of the integrated air concentration, it is possible to obtain relationships between environmental concentrations and retrospective human health risk in which time is not an explicit variable. The following discussion develops these relationships between dose and environmental concentrations on untracked and tracked floors, walls and ceilings, for HVAC filters, and for human nasal passages. The air compartment is not considered here as concentrations decline rapidly in this compartment and do not represent accumulated dose.⁽¹⁸⁾

The concentration of *B. anthracis* on the untracked floor is the integrated number of spores deposited over time ($t_a - t_b$), divided by the area of the untracked floor, A_{uf} :

$$C_{uf} = \frac{M_{uf}}{A_{uf}} = \frac{\lambda_{uf}V}{A_{uf}} \int_{t_a}^{t_b} C_{air}(t)dt. \quad (7)$$

Assuming that the occupants of the room have experienced the exposure from the beginning (a health-protective assumption as discussed above), which can be expressed mathematically as $t_1 = t_a = 0$ and $t_2 = t_b$, one can combine Equations (2) and (7) to link the dose with the concentration on untracked horizontal surfaces:

$$\frac{A_{uf}C_{uf}}{\lambda_{uf}V} = \int_0^{t_b} C_{air}(t)dt = \frac{\text{dose}}{I}. \quad (8)$$

The deposition rate onto the untracked floor for *B. anthracis* (λ_{uf}) is a function of the deposition area, volume of the room, and the deposition velocity (v_{uf} , units of m/s):⁽⁴¹⁾

$$\lambda_{uf} = \frac{v_{uf}A_{uf}}{V}. \quad (9)$$

Thus Equation (8) can be rewritten as:

$$\text{dose} = I \frac{C_{uf}}{v_{uf}}. \quad (10)$$

At low doses, Equation (10) can be combined with Equation (5), the Taylor series approximation of an exponential dose-response function, to link the probability of mortality with the concentration of *B. anthracis* on the untracked floor:

$$\text{risk} \approx rI \frac{C_{uf}}{v_{uf}}. \quad (11)$$

If a beta-Poisson dose-response function is used, then Equation (6) is used in place of Equation (5):

$$\text{risk} \approx \frac{\alpha}{\beta} I \frac{C_{uf}}{v_{uf}}. \quad (12)$$

At high doses, the exact form of the dose-response model must be used rather than the Taylor series approximations:

$$\text{risk} = 1 - e^{-rI \frac{C_{uf}}{v_{uf}}}, \quad (13)$$

$$\text{risk} = 1 - \left(1 + I \frac{C_{uf}}{v_{uf}\beta}\right)^{-\alpha}. \quad (14)$$

For the walls and ceilings, which are assumed not to be subject to substantial resuspension, one need only replace C_{uf} , v_{uf} by C_w , C_{ce} and v_w , v_{ce} in these

equations in order to relate surface concentration to risk. Strictly speaking, Equations (10)–(14) do not require the assumption of uniform mixing in the air compartment. The surface concentration might be related to the air concentration immediately adjacent to the surface. It is when this air concentration is assumed to apply generally to the occupants of the room that the assumption of complete mixing is required.

For the HVAC filter, a relationship can be developed by first noting that the concentration of *B. anthracis* on the filter (C_f) is defined as the accumulated mass of *B. anthracis* on the filter divided by the area of the filter:

$$C_f = \frac{M_f}{A_f} = \frac{epQ}{A_f} \int C_{air}(t)dt. \quad (15)$$

Combining Equations (2) and (15) produces a relationship between dose and filter concentration:

$$\frac{A_f C_f}{epQ} = \int C_{air}(t)dt = \frac{\text{dose}}{I},$$

$$\text{dose} = I \frac{A_f C_f}{epQ}. \quad (16)$$

For low risks, Equation (16) can be substituted into Equations (5) and (6) to obtain an estimate of risk as a function of the concentration of *B. anthracis* on the HVAC filter:

$$\text{risk} = rI \frac{A_f C_f}{epQ}, \quad (17)$$

$$\text{risk} = \frac{\alpha}{\beta} I \frac{A_f C_f}{epQ}. \quad (18)$$

For higher doses, one would need to substitute Equation (16) into the full dose-response function, Equation (3) or Equation (4), respectively.

Relating the concentration of *B. anthracis* on the tracked floor to risk is more complicated as the tracked floor concentration is not simply the integral of the air concentration but reflects losses due to resuspension and, strictly speaking, there is not a functional relationship between surface concentration and risk. However, one can neglect the resuspension if its effects on concentration are minor compared to deposition. This is the case initially (air concentrations are high resulting in high deposition while surface concentrations are low resulting in low resuspension). Thus, if samples are collected soon after release, resuspension may be neglected and Equations (11) and (12), which were derived for untracked surfaces, could be applied as approximate

relationships for tracked surfaces. From a practical viewpoint, one would seek to set a boundary on the time period within which samples from tracked surfaces would be considered valid indicators of risk. For example, one might set a threshold that when the change of surface concentration due to resuspension is less than 5%, one can assume that deposition is the dominant process within that period. A conservative method of estimating loss to resuspension is to assume that all the spores are deposited at $t = 0$ and that there is no redeposition after resuspension occurs. In this situation:

$$\frac{C}{C_0} = e^{-\mu t} = 0.95, \quad (19)$$

where C_0 is the total *B. anthracis* spores' initial concentration on tracked floor and C is the *B. anthracis*' concentration on the tracked floor at time = t . This method is conservative in that it will overestimate the loss due to resuspension and hence underestimate the time at which losses remain below the 5% threshold. Based on resuspension rates from the literature (Table I^(5,12,33,41,44-46,54,55,57,62-69)), to change surface concentrations by 5% will take almost 427, 27, 64, and 13 hours for spores with diameter 1, 3, 5, and 10 μM , respectively. Thus, for the larger diameter particles, samples would need to be collected within several hours of the release, while for smaller diameter particles concentrations would be relatively stable for several days.

For human nasal passages, the concentration of *B. anthracis* is defined as the accumulated mass of *B. anthracis* divided by the area of the nasal passage:

$$C_n = \frac{M_n}{A_n} = \frac{Ie_n}{A_n} \int C_{\text{air}}(t) dt, \quad (20)$$

where e_n is the nasal passages particle remove efficiency and A_n is nasal passage area. Combining Equations (2) and (20) provides the link between dose and C_n :

$$\frac{A_n C_n}{Ie_n} = \int C_{\text{air}}(t) dt = \frac{\text{dose}}{I}.$$

For low doses and an exponential dose-response function, the risk can be related to nasal concentration by:

$$\text{risk} = r \frac{A_n C_n}{e_n}. \quad (21)$$

For the beta-Poisson dose-response function, α/β would replace r , while for higher risk levels the dose would need to be substituted into the full dose-response expression.

3.3. Prospective Risk

In the prospective scenario, the risk is related to the concentration of *B. anthracis* on the tracked floor under the assumptions that spores from other surfaces are not reaerosolized, the *anthracis* initially present in the air has had time to dissipate, the exposure time is infinite, and that there is no loss of viability over time (see discussion of assumptions above). The inhaled dose is determined by integrating Equation (2) with C_{air} expressed as mass of *B. anthracis* spores in the air compartment (see Equation (A-3) in the Appendix) divided by volume of the room:

$$\text{dose} = I \int_0^\infty C_{\text{air}}(t) dt = \frac{I}{V} \left[\frac{c_1 v_{1,1}}{D_1} e^{D_1 t} + \frac{c_2 v_{1,2}}{D_2} e^{D_2 t} \right]_0^\infty, \quad (22)$$

where $D_1, D_2, v_{1,1}, v_{1,2}, v_{2,1}$, and $v_{2,2}$ c_1 and c_2 are all constants (see Appendix for definitions). When time goes to infinity, the inhaled dose will be:

$$\text{dose} = -\frac{I}{V} \left[\frac{c_1 v_{1,1}}{D_1} + \frac{c_2 v_{1,2}}{D_2} \right]. \quad (23)$$

Substituting c_1 and c_2 for the prospective scenario (see Appendix for detail), expressing the initial mass as the product of $C_{\text{tf},0}$ and A_{tf} where A_{tf} is the area of the tracked floor, and substituting into the low dose approximation of the exponential dose-response function yields:

$$\text{risk} = r C_{\text{tf},0} A_{\text{tf}} \frac{I}{V} \frac{(D_2 - D_1) v_{1,2} v_{1,1}}{D_1 D_2 (v_{1,1} v_{2,2} - v_{1,2} v_{2,1})}. \quad (24)$$

As with the retrospective case, for a beta-Poisson dose-response function, α/β would replace r , and at high doses, the full dose-response expressions would have to be used. In order to simplify the risk expression, we introduce a new constant Γ , the future risk coefficient (unit of s):

$$\Gamma = \frac{(D_2 - D_1) v_{1,2} v_{1,1}}{D_1 D_2 (v_{1,1} v_{2,2} - v_{1,2} v_{2,1})}, \quad (25)$$

which is a function of characteristics known before an incident (deposition rates, filter efficiency, recycle proportion, room dimensions, and ventilation rate). Values for Γ (steady state) for our model office suite are presented in Fig. 2. The future risk coefficient for other common building configurations could be computed and tabulated before an incident, and one could then use Γ as a constant of proportionality to relate surface concentration to risk.

Table I. Model Inputs

Symbol	Meaning	Units	Value	Source
V	Room dimensions	m ³	5.6 × 5.6 × 2.5	Assumed a typical office based on (5–54)
A _{tf}	Area-tracked floor	m ²	5.6 × 5.6 × 0.75	
A _{utf}	Area-untracked floor	m ²	5.6 × 5.6 × 0.25	
A _{ce}	Area ceiling	m ²	5.6 × 5.6	
A _w	Area wall	m ²	5.6 × 2.5 × 4	
A _f	Filter area	m ²	3.82 × 10 ⁻² (2.81 × 10 ⁻² –5.62 × 10 ⁻²)	Q/A = 137m/min (91–183 m/min)
A _n	Area of nasal passages	m ²	0.8	(62)
ACH	Air changes per hour		4	(63)
Q	Discharge	m ³ /s	0.087	Q = V × ACH/3600 (in seconds)
f	Proportion tracked		0.75	(63)
μ ₂	Resuspension rate	s ⁻¹	D = 1 μM D = 3 μM D = 5 μM D = 10 μM	3.3 × 10 ⁻⁸ 5.3 × 10 ⁻⁷ 2.2 × 10 ⁻⁷ 1.1 × 10 ⁻⁶ (5, 41)
e	Filter efficiency		D = 1 μM D = 3 μM D = 5 μM D = 10 μM	0.098 0.49 0.74 0.88 (5)

Value Scale

Symbol	Meaning	Units	Diameter	Value Scale				Input Value
				Lower Bound	Source	Upper Bound	Source	
V _{uf} , V _{tf}	Deposition velocity on untracked and tracked floor	m/s	1 μM	3.5 × 10 ⁻⁵	(64)	8.0 × 10 ⁻⁴		6.9 × 10 ⁻⁵
			3 μM	2.0 × 10 ⁻⁴	(57)	6.0 × 10 ⁻³	(57)	4.2 × 10 ⁻⁴
			5 μM	3.0 × 10 ⁻⁴		1.4 × 10 ⁻²	(65)	1.4 × 10 ⁻³
			10 μM	7.0 × 10 ⁻⁴		2.7 × 10 ⁻²		5.6 × 10 ⁻³
V _w	Deposition velocity on walls	m/s	1 μM	3.5 × 10 ⁻⁸	(64)	9.0 × 10 ⁻⁵	(66)	3.9 × 10 ⁻⁵
			3 μM	1.5 × 10 ⁻⁸		2.1 × 10 ⁻⁴		1.6 × 10 ⁻⁴
			5 μM	1.0 × 10 ⁻⁸		4.0 × 10 ⁻⁴		3.1 × 10 ⁻⁴
			10 μM	7.0 × 10 ⁻⁹		6.0 × 10 ⁻⁴		3.5 × 10 ⁻⁴
V _{ce}	Deposition velocity on ceiling	m/s	1 μM				(57)	6.2 × 10 ⁻⁷

Value Scale

Symbol	Meaning	Diameter	Value Scale					Source
			Lower Bound	Source	Upper Bound	Source	Input Value	
e _n	Nasal passages particle remove efficiency	1 μM	0.02		0.25		0.14	
		3 μM	0.22	(64)	0.68	(67)	0.45	Midpoint of range
		5 μM	0.42		0.81		0.62	
		10 μM	0.62		0.91		0.77	
r	Probability of a single <i>Bacillus anthracis</i> spore initiating infection	1–5 μM	9.1 × 10 ⁻⁷	(33)	7.0 × 10 ⁻⁵	(33)	7.2 × 10 ⁻⁶	(12)
α/β		10 μM	1.0 × 10 ⁻⁷	Extrapolated from (33)	8.1 × 10 ⁻⁶	Extrapolated from (33)	8.2 × 10 ⁻⁷	(12)
Risk	Acceptable risk level		1.0 × 10 ⁻⁵	(68)	1.0 × 10 ⁻³	(69)	1.0 × 10 ⁻⁴	Midpoint of range
I	Breathing rate	m ³ /hr	0.8	(55)	2.0	(55)	1.02	(55)
p	Recirculation fraction		0	(63)	1	(63)	0.8	(5)
d _c	Fractal dimension		1.1	(44–46)	3	(44–46)	2	(44–46)

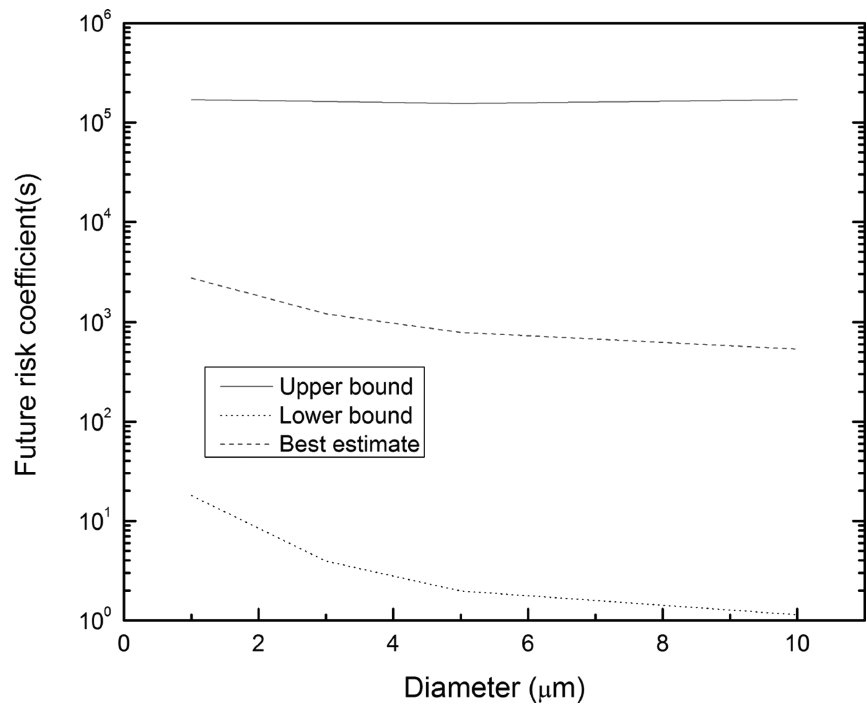


Fig. 2. Future risk coefficient for different diameters of *B. anthracis* spores.

3.4. Concentration Standard for a Mixture of Particle Sizes

Thus far, different diameters have been treated separately. In reality, a release will consist of a mixture of particle sizes, and it may be useful to set a single concentration standard that reflects an aggregate risk from the different particular sizes present. In this analysis, it is assumed that the relative fraction of different particle sizes present is known, although in reality further work may be needed to develop either analytical methods or inverse modeling approaches to effectively identify size fraction.

The approach presented here is applicable for standards based on low risk levels, where total risk can be expressed as the sum of the risks presented by the different size fractions and the risk of each size fraction is proportional to the concentration (i.e., the Taylor series approximations to the dose-response functions are valid):

$$risk_{total} = Conc_{total,S} (f_1 \Omega_1 + f_3 \Omega_3 + f_5 \Omega_5 + f_{10} \Omega_{10}), \tag{26}$$

where f_i represents the fraction of total *B. anthracis* spores with diameter i and Ω is the constant of proportionality for size fraction i (for the prospective case Ω could be retrieved from Equation (24) while for the retrospective case can be obtained by inspecting any equation from Equations (11), (17), or (21)

for exponential dose-response function, and with r replaced by α/β in cases where the beta-Poisson dose-response function is applicable).

From a regulatory standpoint, it is customary to establish concentration standards, not constants of proportionality. If concentration standards for different size fractions are established that correspond to a given risk level, then these standards may be adapted to different particle size mixtures by noting that Ω is simply the ratio of the concentration standard to the specified risk level. Thus:

$$risk_{total} = Conc_{total,S} \left(f_1 \frac{risk_1}{stn_{1,S}} + f_3 \frac{risk_3}{stn_{3,S}} + f_5 \frac{risk_5}{stn_{5,S}} + f_{10} \frac{risk_{10}}{stn_{10,S}} \right), \tag{27}$$

where $risk_i$ is the specified risk level $stn_{i,S}$ the concentration standard applicable to size fraction i on surface S . When the risk levels associated with all the standards are the same, then a joint concentration standard can be calculated from the individual size fraction standards as follows:

$$Conc_{total,S} = \frac{1}{\frac{f_1}{stn_{1,S}} + \frac{f_3}{stn_{3,S}} + \frac{f_5}{stn_{5,S}} + \frac{f_{10}}{stn_{10,S}}}. \tag{28}$$

3.5. Minimum Sampling Area

The surface concentrations corresponding to acceptable risk levels are likely to be very low. This raises the question as to whether a negative test result provides sufficient basis for concluding that the risk is below the desired standard. The following discussion considers how to interpret negative sampling results to assess compliance with a standard. Such data might be generated by culture methods (either plate counts or most probably number methods) or by qPCR. The discussion first assumes that a single spore is present in each particle, and then considers the impacts of clumping on the results. For the culture methods, it is assumed that clumps of spores are broken apart during the extraction procedure. For qPCR, it is assumed that recovery fractions are the same for clumped and unclumped spores. For a more complete discussion of the sampling methods and issues involved in environmental detection of *B. anthracis* spores, see Herzog *et al.*⁽⁴²⁾

3.5.1. No Clumping

From a classical statistical point of view, one wishes to reject the hypothesis that the concentration exceeds the standard with a sufficient level of confidence $1 - \alpha$. If one assumes that a single spore is detectable and that the spores are distributed on the surface according to a Poisson distribution⁽⁴³⁾ with a mean equal to the product of A and C_{stan} where A is the area sampled, and C_{stan} is the surface concentration standard, then one can reject the hypothesis:

$$H_0: \text{Concentration} > C_{\text{stan}}.$$

Given a negative sampling result when:

$$\text{Prob}(x = 0) = e^{-AC_{\text{stan}}} < \alpha, \quad (29)$$

where x is the number of organisms found in the area sampled.

In many cases, there is a minimum number of organisms required for detection, in which case Equation (29) becomes:

$$\text{Prob}(x < DL_{\text{eff}}) < \alpha, \quad (30)$$

$$\sum_{x=0}^{DL_{\text{eff}}-1} \frac{e^{-(AC)}(AC)^x}{x!} < \alpha,$$

where DL_{eff} is the effective detection limit, assumed here to be 11 spores for PCR. (Herzog *et al.*⁽⁴²⁾ indicate that instrument detection limits for qPCR may

be as low as 10 cells per ml, although actual environmental detection limits may be orders of magnitude higher). The approach allows some realism in that small numbers of spores will be difficult to detect, and accounts for one important source of variability in detection of microorganisms, sample variability in their occurrence. However, this approach does assume a deterministic threshold of detection. In reality, this threshold of detection DL_{eff} may be variable. Future efforts to refine this approach could include developing appropriate distributions for DL_{eff} and making DL_{eff} a function of sample size or other characteristics (e.g., degree of interferences present).

3.5.2 Clumping Occurs

The previous section assumes that spores do not clump together. If clumping occurs, then one may assume that the clumps, not the individual spores, are Poisson distributed. Both the surface concentrations and DL_{eff} must be revised to reflect the detectable number of clumps by dividing by the number of spores in a clump (N_δ where δ references the diameter of the clump). Table VI presents ranges for the number of spores in a clump, which are calculated by first estimating the volume of an aggregated particle:⁽⁴⁴⁾

$$V_\delta = \frac{\pi^{F/2}}{\Gamma(1 + F/2)} \times r^F, \quad (31)$$

where V_δ is the volume of a clumped particle with diameter $\delta \mu\text{M}$, r is the radius for the aggregated particle, F is fractal dimension whose values are between 1.1 and 3 under different aggregation scenarios,^(45,46) and $\Gamma(F)$ is the Γ function. The number of spores per clump is determined by dividing by the volume of a single spore ($1 \mu\text{M}$ in this study):

$$N_\delta = \frac{V_\delta}{V_1}. \quad (32)$$

Thus minimum sampling area for clumped particles is calculated from Equation (33):

$$\sum_{X=0}^{DL_{\text{eff}}/N_\delta - 1} \frac{\left(\frac{A}{N_\delta} C\right)^X}{X!} e^{-\left(\frac{A}{N_\delta} C\right)} < \alpha. \quad (33)$$

The detection limit DL_{eff}/N_δ should be rounded up to the nearest integer to reflect the number of clumps required to produce a detectable signal.

To verify adherence with the standard for a mixture of sample sizes, one would have to demonstrate $\text{Prob}(x < DL_{\text{eff}}) < \alpha$. However, x would not follow a

simple distribution but would be a mixture of Poisson distributions for the different clump sizes. For high detection limits, a normal approximation would be appropriate while for low detection limits one would have to exhaustively enumerate all combinations of clump sizes capable of producing nondetectable results:

$$\sum \text{prob}[x_1 = a] \text{prob}[x_3 = b] \times \text{prob}[x_5 = c] \text{prob}[x_{10} = d] < \alpha, \quad (34)$$

where the sum is taken over all combinations of clumped particles for which:

$$N_1x_1 + N_3x_3 + N_5x_5 + N_{10}x_{10} < DL_{\text{eff}}.$$

3.5.3. Imperfect Sampling Recovery

This approach can be broadened to handle recoveries that are below 100%. In this case, the mean of the Poisson process becomes $A C R_e$ where R_e is the recoverable fraction of the spores. Thus in the case of a constant recovery Equation (33) is modified to:

$$\sum_{X=0}^{\frac{DL_{\text{eff}}}{N_\delta} - 1} \frac{\left(A \frac{C}{N_\delta} R_e \right)^X e^{-A \frac{C}{N_\delta} R_e}}{X!} < \alpha. \quad (35)$$

Thus for a constant recovery, one identifies the value of the product $A \frac{C}{N_\delta} R_e$, which produces the desired α . In reality, there is likely substantial uncertainty in the recovery fraction. As R_e is bounded by 0 and 1, a beta distribution is a natural choice to represent variability and uncertainty. Based on a review of the literature,^(24,25,42,47–52) parameters of alpha = 1.87 and beta = 2.85 were selected by fitting the recovery efficiencies reported in the above mentioned studies using BestFit software (Palisade, New York, NY) (median recovery = 0.38, 5th percentile = 0.089, 95th percentile = 0.76). The use of a common distribution here ignores differences based on sample collection method, particle size, surface type, particle surface charge, etc. Clearly, further work addressing these factors is warranted. Given the specified distribution of R_e , Monte Carlo methods were used to determine the value of AC/N_δ required to obtain a detectable number of clumps of spores with 95% confidence, and these values are listed in Table VI (values were simulated using Matlab software, Mathwork, Natick, MA). Thus one can divide the values for “Expected number of particles (area ×

concentration/ N_δ)” given in Table VI by C/N_δ , to estimate the required sampling area.

In all cases, it is assumed that the concentration is uniform over the sampled area A . This is convenient mathematically, but if this is not true then the sampling areas calculated here would not be health protective. In the event of spatial heterogeneity in concentration, the number of microorganisms detected would no longer follow a Poisson distribution. A negative binomial distribution is frequently used to model microbial count data that show greater than Poisson variability, and in this case Equations (29), (30), and (33) can be reworked with the cumulative probability of a negative binomial distribution (or other appropriate distribution) substituted for the cumulative Poisson. The major complication that this entails is that for the binomial distribution the variance can be adjusted independent of the mean. In the absence of detectable counts, there is no way to estimate the variance from the data, and values would have to be assumed. An example analysis of this approach is provided by Hong.⁽⁵³⁾ Future work should be directed toward developing appropriate variance values from modeling or field testing.

4. EXAMPLE APPLICATION

This section presents example calculations based on a hypothetical office equipped with a simple HVAC system. Numerical values of model input parameters are provide in Table I and Figs. 3 and 4 describe the range of deposition velocities on floors and walls for various diameters and the range of nasal passages particle remove efficiency, respectively. Recirculation rate (Q) is based on an assumed value of 4 air changes per hour and a recirculation fraction of 80%. The surface area of the filter is computed by assuming a flow rate of 450 ft/min (300–600 ft/min range is typical)⁽⁵⁴⁾ or 137 m/min to the HVAC filter. Breathing rate is highly variable and depends on many factors including the health of an individual and activity level. We assume a breathing rate of 1.02 m³/hour corresponding to medium activity.⁽⁵⁵⁾ This is conservative for an office building where physical activity levels for many occupants are low. Separate dose-response parameters are used for *B. anthracis* spores with diameters of 1–5 μM (which are considered respirable) and for spores in the 10 μM category (which are less respirable). Uncertainties in these numbers should include not just sample variability from a single dosing experiment but should include uncertainty associated with variability in host

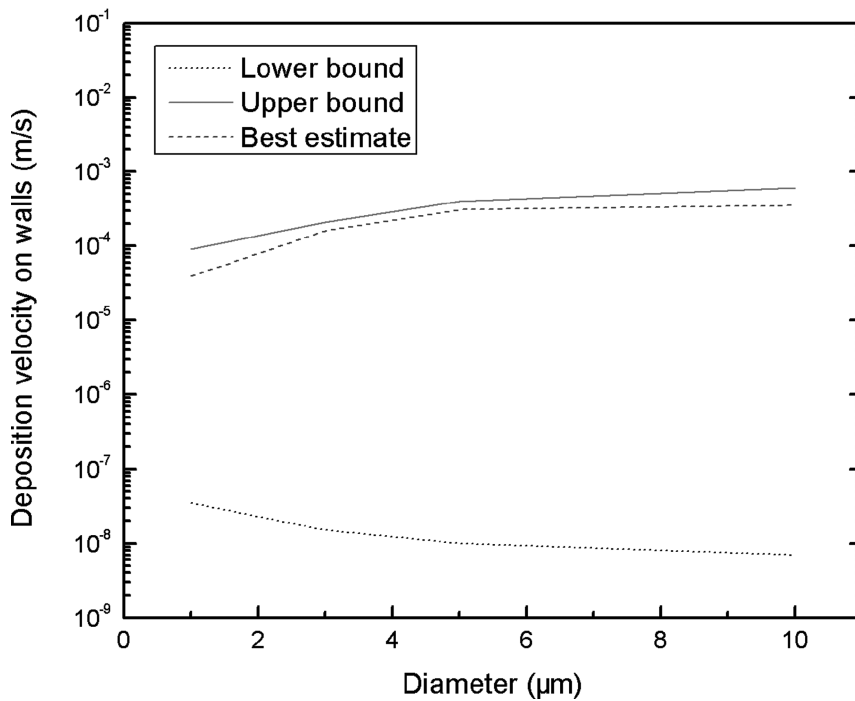
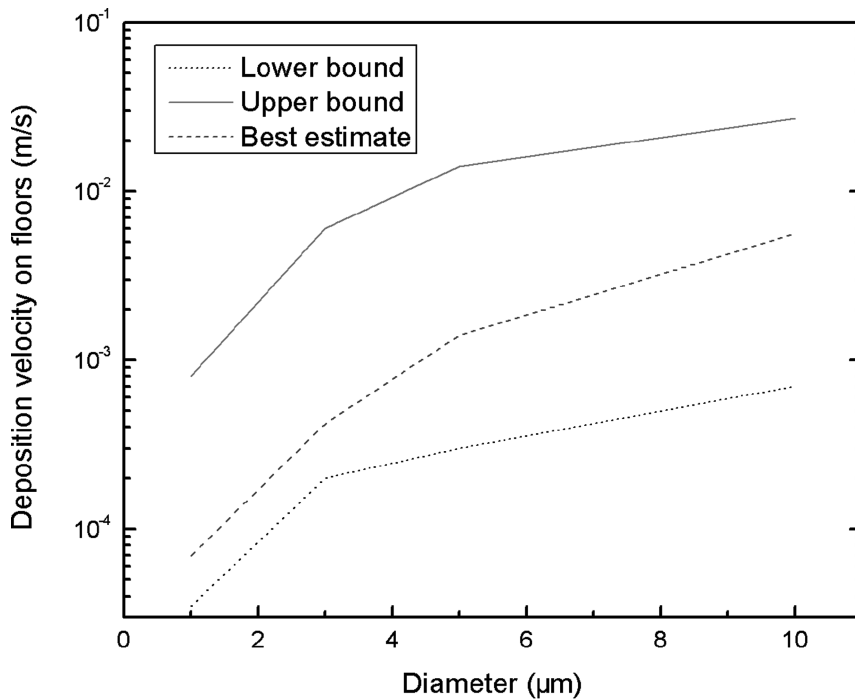


Fig. 3. Scale of deposition velocity on floors and walls versus particle diameter.

species sensitivity and pathogen strain infectivity. For the respirable spores, the results of the meta-analysis of Mitchell-Blackwood *et al.*,⁽³³⁾ which considered variability among a set of three dose-response experiments that employed different host species and *B. an-*

thraxis strains, are used to set uncertainty bounds for dose-response. Mitchell-Blackwood *et al.*⁽³³⁾ did not include an assessment of larger diameter spore dose response. In this study, the uncertainty factor that Mitchell-Blackwood *et al.* developed for the smaller

Fig. 4. Nasal passages removal efficiency versus particle diameter.

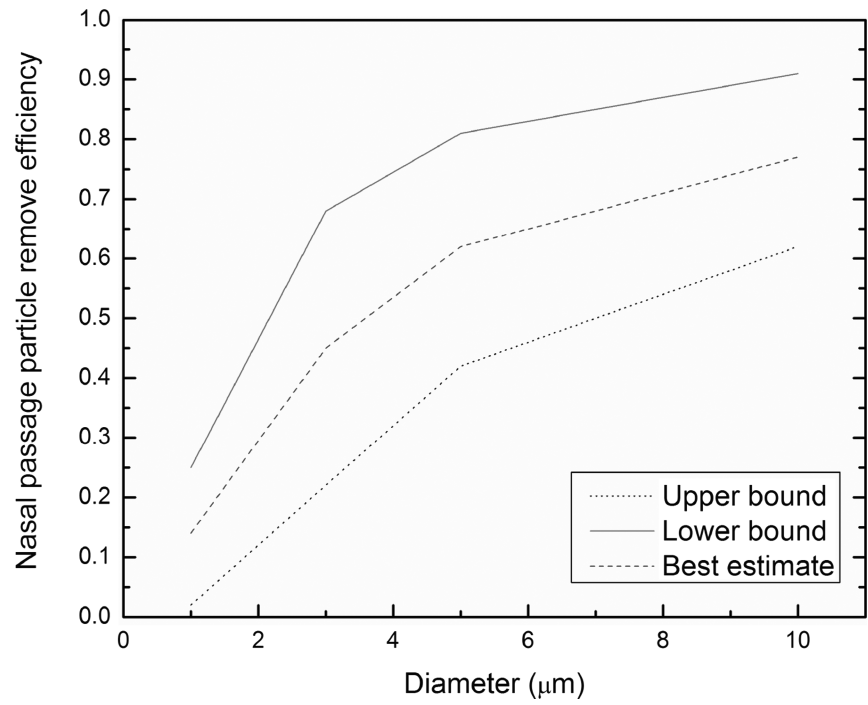
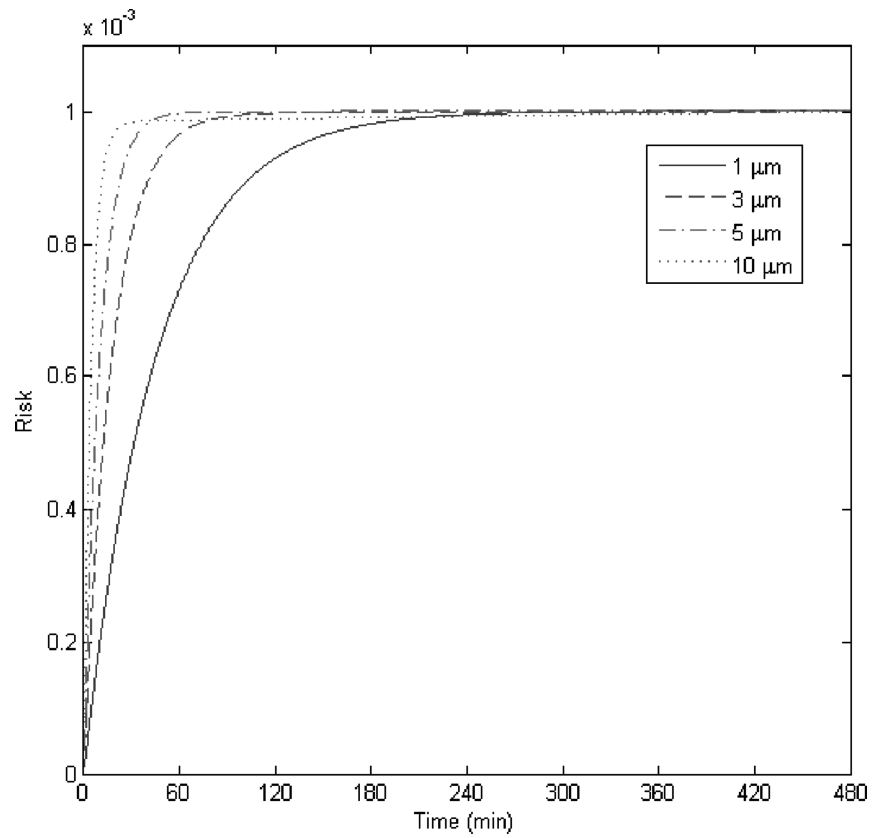


Fig. 5. Retrospective risk versus time for an ultimate risk of 10^{-3} . (Quantities are shown in Table III.)



size fractions is assumed to be applicable to the 10 μM fraction.

4.1. Retrospective Risk

In this scenario, we assume that *B. anthracis* spores were released into the air compartment. Fig. 5 shows the relationship between risk of mortality and time for different particle sizes. This plot is intended to provide guidance on the time-scale over which the approach presented here may be usefully applied. The plot shows that risk increases rapidly at first and then approaches an asymptote as the air concentration declines. Risks caused by particles with diameters of 3, 5, and 10 μM approach an asymptote after 1.5 hours while it requires roughly 4 hours for the risk from 1 μM spores to approach its upper bound. This indicates that retrospective risk has a time-scale of roughly a day or less. If the individual is present the majority of a working day (8 hours) then risk estimates are not very sensitive to the time of subsequent sample collection because most of the risk accrues in less than 8 hours.

Table II shows environmental *B. anthracis* concentrations corresponding to a risk level of 1 in 1,000. The use of a time-integrated approach (e.g., Equation (2)) means that the risk values developed here are not for specific time periods but for aggregate exposure, but as discussed above 8 hours is a reasonable time-scale for retrospective exposure and this time period was used in the numerical calculations shown here. If suitable parameters can be identified in advance of a release, then surface concentrations can be related to risk using simple plots such as Fig. 6. The ranges shown in Table II are based on the maximum range found from a series of one variable sensitivity analyses.⁽⁵⁶⁾ Specifically, the upper and lower bounds for deposition velocity, dose response, inhalation rate, HVAC system flow rate (Q/A_f), recirculation fraction, and nasal passage removal efficiency (given in Table I) were used to calculate environmental concentrations with all other parameters retained at their nominal values. The widest of the ranges from the single variable analyses are reported in Table II.

Table III shows the required sampling area with perfect and imperfect sampling recovery efficiency (spore clumping has been taken into account with the AC/N_δ values from Table VI) required for a negative result to indicate conformance with the 10^{-3} risk level. Ranges in this table reflect the ranges for the concentration values given in Table II.

Table II. The Environmental Concentrations of *B. anthracis* Corresponding to a Retrospective Inhalation Risk of 10^{-3} ($t = 480$ min)

Diameter (μM)	Amount of Initial Release	Concentration (Spores/ m^2)									
		Range	Tracked (Untracked) Floor	Range	Walls	Range	Filter	Range	Nasal Passages	Range	
1	1.4×10^4	$2.4 \times 10^3 - 1.9 \times 10^5$	35	$9.0 \times 10^{-1} - 4.0 \times 10^3$	20	$9.0 \times 10^{-4} - 4.5 \times 10^2$	9.2×10^4	$0^* - 1.5 \times 10^6$	26	$0.36 - 3.4 \times 10^2$	
3	3.6×10^4	$2.5 \times 10^3 - 1.2 \times 10^6$	2.1×10^2	$5.1 - 3.0 \times 10^4$	83	$3.9 \times 10^{-4} - 1.0 \times 10^3$	4.6×10^5	$0^* - 7.4 \times 10^6$	82	$3.9 - 9.3 \times 10^2$	
5	6.4×10^4	$2.7 \times 10^3 - 2.6 \times 10^6$	7.5×10^2	$7.6 - 6.9 \times 10^4$	1.7×10^2	$2.6 \times 10^{-4} - 2.0 \times 10^3$	7.3×10^5	$0^* - 1.1 \times 10^7$	118	$7.5 - 1.1 \times 10^3$	
10	1.2×10^6	$2.6 \times 10^4 - 4.3 \times 10^7$	2.4×10^4	$1.6 \times 10^2 - 1.2 \times 10^6$	1.7×10^3	$1.6 \times 10^{-3} - 2.7 \times 10^4$	7.7×10^6	$0^* - 1.2 \times 10^8$	1.3×10^3	$96 - 1.1 \times 10^4$	

Notes: All inputs are based on Table I. Range based on maximum and minimum of sensitivity analysis. Concentrations of *B. anthracis* are not shown because no quantified ceiling deposition rate was found in the literature for diameter larger than 1 μM . The lowest value for the concentration of filter is zero when there is no return air after being filtered by the HVAC system.

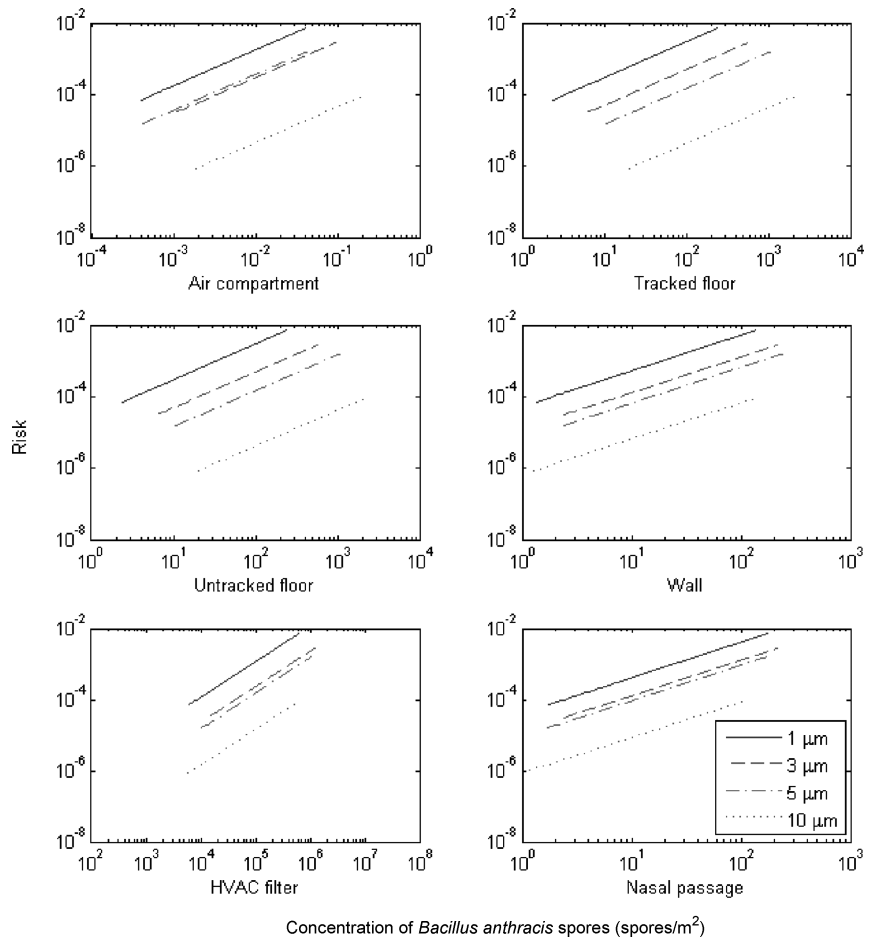


Fig. 6. Retrospective risk versus surface concentration after an 8-hour exposure following an instantaneous release (quantity is between 1,000–100,000 spores).

4.2. Prospective Risk

In this scenario, *B. anthracis* spores are initially present on the tracked surface and the resuspension process causes the spores to reenter the air. Fig. 7 shows the accumulated risk over time. Clearly, the time-scale is much slower for prospective risk than for retrospective risk. Whether the full risk shown here will actually be achieved is uncertain as this would require fairly vigorous, continual resuspension, and continuous inhabitation at the same residence for many years. In addition, it is not clear that spores would survive for such extended periods of time in the indoor environment or that they would continue to be so readily reaerosolized as they may tend to bind irreversibly with surfaces over time.^(31,32) These estimates are presented as health-protective estimates that can be refined by further study of spore viability and reaerosolization over time. Table IV shows the concentration of *B. anthracis* corresponding to a risk level of 10⁻³ (spore clump-

ing has not been taken into account with the nominal values from Table VI). As with the retrospective approach, risks are time-integrated; using an exposure period of five years for the numerical calculations allows exposure associated with a single release to reach its asymptote.

It is noteworthy that the prospective risk standards developed here are considerably less stringent than the retrospective standards. While 35 spores per m² (diameter = 1 μM) on the floor would indicate a retrospective risk of 1/1,000 (Table II), 600 spores per m² (diameter = 1 μM) are required to produce a prospective risk of 1/1,000. The same release will produce 17 times greater retrospective risk than prospective risk for 1 μM spores, 6.7 times greater retrospective risk for 3 μM spores, 2.8 times greater risk for 5 μM spores, and 1.1 times greater risk for 10 μM spores.

Table V shows the sampling area (spore clumping has been taken into account) required for a negative result to indicate conformance with the 10⁻³

Table III. Minimum Sampling Area Corresponding to a 10^{-3} Inhalation Risk for Retrospective Exposure Estimation ($t = 480$ min)

Diameter (μM)	Recovery Efficiency	Tracked (Untracked)		Sampling Area (m^2)					
		Floor	Range	Walls	Range*	Filter	Range	Nasal Passages	Range
1	100%	4.9×10^{-1}	4.3×10^{-3} -19	8.5×10^{-1}	3.8×10^2 - 1.9×10^4	1.8×10^{-4}	1.1×10^{-5} -inf	6.5×10^{-1}	5.0×10^{-2} -47
	<100%	3.6	3.2×10^{-2} - 1.4×10^2	6.4	2.8×10^3 - 1.4×10^5	1.4×10^{-3}	8.5×10^{-5} -inf	4.9	3.7×10^{-1} - 3.6×10^2
3	100%	1.6×10^{-1}	4.8×10^{-4} - 1.3×10^1	4.0×10^{-1}	1.4×10^{-2} - 1.7×10^5	7.3×10^{-5}	1.9×10^{-6} -inf	4.1×10^{-1}	1.5×10^{-2} - 1.7×10^1
	<100%	8.7×10^{-1}	2.6×10^{-3} - 7.1×10^1	2.2	7.8×10^{-2} - 9.3×10^5	4.0×10^{-4}	1.1×10^{-5} -inf	2.2	8.4×10^{-2} - 9.3×10^1
5	100%	8.0×10^{-2}	2.6×10^{-4} - 2.6×10^1	3.5×10^{-1}	9.0×10^{-3} - 7.5×10^5	8.2×10^{-5}	1.6×10^{-6} -inf	5.1×10^{-1}	1.6×10^{-2} - 2.6×10^1
	<100%	4.0×10^{-1}	1.3×10^{-3} - 1.3×10^2	1.8	4.5×10^{-2} - 3.8×10^6	4.1×10^{-4}	8.2×10^{-6} -inf	2.5	8.2×10^{-2} - 1.3×10^2
10	100%	9.9×10^{-3}	3.3×10^{-5} -9.8	1.4×10^{-1}	1.4×10^{-3} - 9.8×10^5	3.1×10^{-5}	1.6×10^{-6} -inf	1.8×10^{-1}	3.5×10^{-3} - 1.6×10^1
	<100%	4.9×10^{-2}	1.6×10^{-4} - 4.9×10^1	7.0×10^{-1}	7.2×10^{-3} - 4.9×10^6	1.5×10^{-4}	1.6×10^{-6} -inf	9.1×10^{-1}	1.8×10^{-2} - 8.1×10^1

Note: We do not show ceiling as a sampling area due to its low concentration, which requires a large sampling area, which is difficult to achieve. The maximum sampling area for walls and filter are unrealistically large due to their relative low or zero concentrations.

risk level for an alpha value of 0.05. Ranges in this table reflect the ranges for the concentration values given in Table IV (which are based on the maximum and minimum values for single variable sensitivity analyses on deposition velocity, dose response, inhalation rate, HVAC system flow rate (Q/A_f), recirculation fraction, and nasal passage removal efficiency).

5. DISCUSSION

This article presents an approach for linking environmental sampling results with human health risk from exposure to *B. anthracis*. This approach is then used to calculate example values for risk-informed concentration standards for both retrospective risk mitigation (e.g., prophylactic antibiotics) and prospective risk mitigation (e.g., environmental clean up and reoccupancy). The results indicate that the same release produces more retrospective risk than prospective risk, and the difference is particularly pronounced for finely aerosolized spores. This indicates that, as with the response to the 2001 attacks, larger areas would be subject to antibiotic treatment of exposed individuals than environmental decontamination.

These results indicate that surface concentrations corresponding to what are sometimes considered *de minimus* levels of risk (10^{-4} through 10^{-6}) would be extremely low. For a 10^{-6} retrospective risk from $1 \mu\text{M}$ particles, the concentration standard for floors would be 0.035 spores/m^2 (i.e., the value in Table II of 35 spores/m^2 for a 10^{-3} risk can be divided by 1,000). Surface sampling to demonstrate compliance with this standard would require that 485 m^2 be sampled, even if 100% collection efficiency could be achieved (Table III value multiplied by 1,000). However, for a risk target of 10^{-4} , then a sample area of 4.9 m^2 is required if 100% recovery is achieved, and 36 m^2 if literature estimates of recoveries are used. These values might be achievable with large-area sampling approaches (large wipes, vacuum filters, etc.) and multiple samples. Values for $10 \mu\text{M}$ particles are much more feasible. For a risk target of 10^{-4} , nearly 0.1 m^2 would be required if 100% recovery is achieved and 0.485 m^2 if literature estimates of recovery are used (Table III values multiplied by 10). Nasal samples and HVAC filter samples may have some role to play in characterizing exposure and risk. Nasal samples have the advantage of directly quantifying personal exposure, but persistence of spores in the nasal environment would need

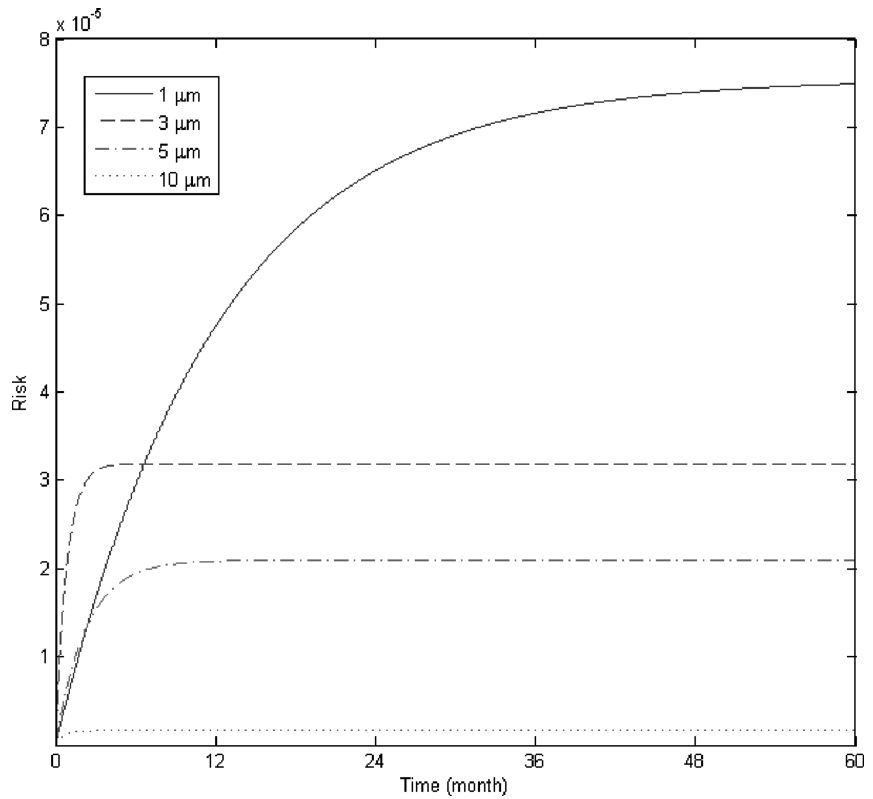


Fig. 7. Prospective risk against time over five years of exposure (quantity is 1,000 spores).

Table IV. Environmental Concentrations of *B. anthracis* Corresponding to a Prospective Inhalation Risk of 10^{-3} ($t = 5$ Years)

Diameter (μM)	Amount of Initial Release (Range)	Concentration (Range) (Spores/ m^2) Tracked Floor
1	1.4×10^4 (2.3×10^2 – 5.0×10^5)	6.0×10^2 (9.8 – 2.1×10^4)
3	3.2×10^4 (1.2×10^3 – 7.3×10^5)	1.4×10^3 (5.1×10^1 – 3.1×10^4)
5	4.9×10^4 (1.7×10^3 – 1.1×10^6)	2.1×10^3 (7.2×10^1 – 4.7×10^4)
10	6.3×10^5 (1.9×10^4 – 1.5×10^7)	2.7×10^4 (8.1×10^2 – 6.4×10^5)

Note: All inputs are based on Table I. Range based on maximum and minimum of sensitivity analysis.

Table V. Minimum Sampling Area on Tracked Floor Corresponding to a 10^{-3} Inhalation Risk for Prospective Exposure Estimation Time = 5 Years

Diameter (μM)	Recovery Efficiency	Best Estimation (m^2)	Range (m^2)
1	100%	2.8×10^{-2}	8.1×10^{-4} – 1.7
	<100%	2.1×10^{-1}	6.0×10^{-3} – 13
3	100%	2.4×10^{-2}	4.6×10^{-4} – 1.3
	<100%	1.3×10^{-1}	2.5×10^{-3} – 7.1
5	100%	2.9×10^{-2}	3.8×10^{-4} – 2.7
	<100%	1.4×10^{-1}	1.9×10^{-3} – 1.4×10^1
10	100%	8.8×10^{-3}	6.1×10^{-5} – 1.9
	<100%	4.4×10^{-2}	3.0×10^{-4} – 9.7

to be better characterized before such samples can be interpreted quantitatively. HVAC filters have considerable potential to concentrate spores and may be an appropriate area for sampling if there is not excessive interference with sampling and analysis from the wide variety of other materials trapped on these filters.

This analysis explicitly calculated clearance-sampling requirements for nondetectable samples. A similar logic may be applied to clearing buildings with detectable concentrations of *B. anthracis* spores. For example, if 11 spores are detected on the floor, then a sampling area of 5.2 m^2 is required for clearance at the 10^{-4} risk level (i.e., one could still reject the hypothesis that $C > 3.5$ spores/ m^2 if one detects 11 spores in 5.2 m^2). Given public concern with anthrax, it is likely that remediation would be

Diameter (μM)	Fractal Dimension (F)		Number of Spores per Particle		Expected Number of Particles (Area \times Concentration/ N_{δ}) Required to Obtain > 10 Spores in 95% of Samples	
	Range	Nominal	Range	Nominal	Perfect Recovery Efficiency ^a	Imperfect Recovery Efficiency ^b
1	NA	2	1	1	≥ 16.96	≥ 128
3	1.1–3	2	3–14	7	≥ 4.8	≥ 26
5	1.1–3	2	6–65	20	≥ 2.99	≥ 15
10	1.1–3	2	13–524	79	≥ 2.99	≥ 15

Table VI. The Ranges of Number of Spores in a Clump

^aCalculated based on Equations (28)–(30).

^bSimulated based on distribution listed in Section 3.5.3. N_{δ} is the number of spores per clump.

undertaken in the case of detectable spores. At a minimum, a much lower alpha value for clearance could be demanded in the case of detected spores. Reducing the alpha value to 0.01 increases the surface sampling size to 6.1 m². In reality, clearance sampling should consist of dispersed samples that would be jointly interpreted to meet the target risk level. While some progress has been made in defining clearance requirements with this work and that of others^(8,57) further work in this area to develop operational plans is warranted.

The ability to reliably sample is a prerequisite for the implementation of environmental standards. For this reason, an initial effort to quantify recoveries based on literature reports was undertaken. A better understanding of what factors influence recoveries is an important topic for future efforts.⁽⁵⁸⁾ There are now several studies available to inform these efforts,^(21,24,25) although knowledge gaps may remain,⁽⁵⁸⁾ particularly for the large sampling areas suggested by this study.

There is great uncertainty in the values calculated here.⁽⁵⁹⁾ Some sources of uncertainty, such as low-dose human response, are likely to be difficult to reduce, given the need to rely on high-dose animal models. However, other sources of uncertainty may be reduced by further efforts. The range of deposition velocities found in the literature was extremely large (Figs. 3 and 4). This range likely reflects variability in room dimensions, materials, and circulation characteristics. To the extent that these characteristics can be mapped to particular deposition rates, it may be possible to decrease the uncertainty in these parameters. This also implies that dif-

ferent concentration standards might be appropriate for different locations (i.e., the correspondence between risk and environmental concentration is site specific because the deposition velocities are site specific).

This analysis relied on a simple uniformly mixed compartment model of environmental transport. A more detailed approach, such as computational fluid dynamics, should be a useful complement to this study. The approach presented in this study serves as a beginning for future analysis. Future research is suggested in the following directions: (1) delineating conditions under which this approach is applicable and conditions under which it is not, (2) identifying surfaces in a room that are most reflective of time-integrated human respired air concentrations, and (3) quantifying and reducing the degree of variance present within a compartment so that confidence limits can be developed that include these smaller scale variations.

ACKNOWLEDGMENTS

This research was funded through the Center for Advancing Microbial Risk Assessment, supported by the U.S. Environmental Protection Agency and U.S. Department of Homeland Security, under the Science to Achieve Results grant program (grant number: R83236201). The authors appreciate valuable discussion and inputs from Syed A. Hashsham, Deb McKean, Sarah Taft, Chuck Haas, Ashley Kenyon, Agami Reddy, and useful comments from anonymous reviewers of this journal.

APPENDIX

Solution to Equation (1)

Equation (1) can be uncoupled, allowing one to solve the subsystem

$$\begin{pmatrix} \dot{M}_{air} \\ \dot{M}_{tf} \end{pmatrix} = \begin{pmatrix} [(1-e)p-1]\frac{Q}{V} - \left(\lambda_{tf} + \lambda_{utf} + \lambda_w + \lambda_{ce} + \frac{Ie_n}{V}\right) & \mu_2 \\ \lambda_{tf} & -\mu_2 \end{pmatrix} \begin{pmatrix} M_{air} \\ M_{tf} \end{pmatrix}, \tag{A-1}$$

by working out the eigenvalues of

$$\begin{pmatrix} [(1-e)p-1]\frac{Q}{V} - \left(\lambda_{tf} + \lambda_{utf} + \lambda_w + \lambda_{ce} + \frac{Ie_n}{V}\right) & \mu_2 \\ \lambda_{tf} & -\mu_2 \end{pmatrix}, \tag{A-2}$$

denoted by D_1 and D_2 , which we suppose are distinct eigenvalues, with corresponding eigenvectors $v_{1,1}$, $v_{1,2}$, $v_{2,1}$, and $v_{2,2}$. The Gerschgorin test shows that the eigenvalues of Equation (A-2) are nonpositive, which verifies that the solutions are stable.⁽⁶⁰⁾

The general solution to the coupled subsystem is:⁽⁶¹⁾

$$M_{air} = c_1 v_{1,1} e^{D_1 t} + c_2 v_{1,2} e^{D_2 t}, \tag{A-3}$$

$$M_{tf} = c_1 v_{2,1} e^{D_1 t} + c_2 v_{2,2} e^{D_2 t}. \tag{A-4}$$

The constants c_1 and c_2 are solved for using the appropriate initial conditions. This process is described for the retrospective and prospective scenarios below. Once M_{air} is obtained from A-3, M_{utf} , M_w , M_f , M_{ce} , and M_n are computed by integrating M_{air} .

Retrospective Case

In the retrospective scenario, the initial conditions are that the mass of *Bacillus anthracis* spores in the air equals the amount of the initial release and the mass of that on the tracked floor is zero, since *Bacillus anthracis* spores are released in the air compartment and are well distributed:

$$t = 0, \longrightarrow \begin{cases} M_{air} = c_1 v_{1,1} e^{D_1 t} + c_2 v_{1,2} e^{D_2 t} = 0 & \text{(a)} \\ M_{tf} = c_1 v_{2,1} e^{D_1 t} + c_2 v_{2,2} e^{D_2 t} = Init & \text{(b)} \end{cases}$$

C_1 can be acquired by canceling C_2 by multiplying Equation (a) by $v_{2,2}$ and subtracting the product of Equation (b) and $v_{1,2}$:

$$\begin{aligned} & (c_1 v_{1,1} v_{2,2} + c_2 v_{1,2} v_{2,2}) - (c_1 v_{1,2} v_{2,1} + c_2 v_{1,2} v_{2,2}) \\ & = Init v_{2,2} - 0, \\ & c_1 (v_{1,1} v_{2,2} - v_{1,2} v_{2,1}) = Init v_{2,2}, \\ & c_1 = \frac{Init v_{2,2}}{v_{1,1} v_{2,2} - v_{2,1} v_{1,2}}. \end{aligned}$$

C_2 also can be acquired in the same manner, multiplying Equation (a) $v_{2,1}$ and subtracting the product of Equation (b) and $v_{1,1}$:

$$\begin{aligned} & (c_1 v_{1,1} v_{2,1} + c_2 v_{1,2} v_{2,1}) - (c_1 v_{1,1} v_{2,1} + c_2 v_{1,1} v_{2,2}) \\ & = Init v_{2,1} - 0, \\ & c_2 (v_{1,2} v_{2,1} - v_{1,1} v_{2,2}) = Init v_{2,1}, \\ & c_2 = \frac{Init v_{2,1}}{v_{2,1} v_{1,2} - v_{1,1} v_{2,2}}. \end{aligned}$$

Prospective Risk

In this scenario, all the *Bacillus anthracis* spores are released on the tracked floor at the beginning. The initial conditions are:

$$t = 0, \longrightarrow \begin{cases} M_{air} = c_1 v_{1,1} e^{D_1 t} + c_2 v_{1,2} e^{D_2 t} = 0 & \text{(c)} \\ M_{tf} = c_1 v_{2,1} e^{D_1 t} + c_2 v_{2,2} e^{D_2 t} = Init & \text{(d)} \end{cases}$$

C_1 can be acquired by multiplying Equation (c) by $v_{2,2}$ and subtracting the product of Equation (d) and $v_{1,2}$:

$$\begin{aligned} & (c_1 v_{1,1} v_{2,2} + c_2 v_{1,2} v_{2,2}) - (c_1 v_{1,2} v_{2,1} + c_2 v_{1,2} v_{2,2}) \\ & = -Init v_{2,2}, \\ & c_1 (v_{1,1} v_{2,2} - v_{1,2} v_{2,1}) = -Init v_{2,2}, \\ & c_1 = \frac{Init v_{2,2}}{v_{2,1} v_{1,2} - v_{1,1} v_{2,2}}. \end{aligned}$$

C_2 also can be acquired in the same path, multiplying Equation (c) $v_{2,1}$ and subtracting the product

of Equation (d) and $v_{1,1}$:

$$\begin{aligned} & (c_1 v_{1,1} v_{2,1} + c_2 v_{1,2} v_{2,1}) - (c_1 v_{1,1} v_{2,1} + c_2 v_{1,1} v_{2,2}) \\ &= -Init v_{1,1}, \\ & c_2 (v_{1,2} v_{2,1} - v_{1,1} v_{2,2}) = -Init v_{1,1}, \\ & c_2 = \frac{Init v_{1,1}}{v_{1,1} v_{2,2} - v_{2,1} v_{1,2}}. \end{aligned}$$

Eigenvalues and Eigenvectors

For simplicity, Equation (A-2) is modified into the following pattern:

$$\begin{pmatrix} W - L & M \\ L & -M \end{pmatrix}, \tag{e}$$

where

$$W = [(1 - e)p - 1] \frac{Q}{V} - \left(\lambda_{uf} + \lambda_w + \lambda_{ce} + \frac{Ie_n}{V} \right)$$

$$L = \lambda_{tf}$$

$$M = \mu_2.$$

The eigenvalues of Equation (e) are listed below:

$$\begin{aligned} D_1 &= -\frac{1}{2}(L + M - W) + \frac{1}{2}(L^2 + 2ML \\ &\quad - 2LW + M^2 + 2WM + W^2)^{\frac{1}{2}}, \\ D_2 &= -\frac{1}{2}(L + M - W) - \frac{1}{2}(L^2 + 2ML \\ &\quad - 2LW + M^2 + 2WM + W^2)^{\frac{1}{2}}. \end{aligned}$$

The eigenvectors of Equation (e) are listed below:

$$v_{1,1} = \frac{-\frac{1}{2}(L - M - W) + \frac{1}{2}(L^2 + 2ML - 2LW + M^2 + 2WM + W^2)^{\frac{1}{2}}}{L},$$

$$v_{1,2} = \frac{-\frac{1}{2}(L - M - W) - \frac{1}{2}(L^2 + 2ML - 2LW + M^2 + 2WM + W^2)^{\frac{1}{2}}}{L},$$

$$v_{2,1} = 1,$$

$$v_{2,2} = 1.$$

REFERENCES

1. Greene CM, Reefhuis J, Tan C, Fiore AE, Goldstein S, Beach MJ, Redd SC, Valiante D, Burr G, Buehler J, Pinner RW, Bresnitz E, Bell BP. Epidemiologic investigations of

- bioterrorism-related anthrax, New Jersey, 2001. *Emerging Infectious Diseases*, 2002; 10:1048–1055.
2. Heller MB, Bunning ML, France MEB, Niemeyer DM, Peruski L, Naimi T, Talboy PM, Murray PH, Pietz HW, Kornblum J, Oleszko W, Beatrice ST. Laboratory response to anthrax bioterrorism, New York City, 2001. *Emerging Infectious Diseases*, 2002; 10:1096–1102.
3. Gurian PL, Small MJ, Lockwood JR, Schervish MJ. Addressing uncertainty and conflicting cost estimates in revising the arsenic MCL. *Environmental Science & Technology*, 2001; 22:4414–4420.
4. EPA. EPA’s Use of Benefit-Cost Analysis: 1981–1986. Washington, DC: Economic Studies Branch Office of Policy Analysis, Office of Policy, Planning and Evaluation, EPA, 1987.
5. Sextro RG, Lorenzetti DM, Sohn MD, Thatcher TL. Modeling the spread of anthrax in buildings. Pp. 506–511 in *Proceedings of Indoor Air 2002*, Monterey, CA.
6. Weis CP, Intrepido AJ, Miller AK, Cowin PG, Durno MA, Gebhardt JS, Bull R. Secondary aerosolization of viable *Bacillus anthracis* spores in a contaminated US Senate Office. *Journal of the American Medical Association*, 2002; 22:2853–2858.
7. Reshetin VP, Regens JL. Simulation modeling of anthrax spore dispersion in a bioterrorism incident. *Risk Analysis*, 2003; 6:1135–1145.
8. Price PN, Sohn MD, Lacomme KSH, McWilliams JA. Framework for evaluating anthrax risk in buildings. *Environmental Science & Technology*, 2009; 6:1783–1787.
9. Huang Y, Haas CN. Time-dose-response models for microbial risk assessment. *Risk Analysis*, 2009; 5:648–661.
10. Huang Y, Bartrand TA, Haas CN, Weir MH. Incorporating time postinoculation into a dose-response model of *Yersinia pestis* in mice. *Journal of Applied Microbiology*, 2009; 3:727–735.
11. Haas CN. On the risk of mortality to primates exposed to anthrax spores. *Risk Analysis*, 2002; 2:189–193.
12. Bartrand TA, Weir MH, Haas CN. Dose-response models for inhalation of *Bacillus anthracis* spores: Interspecies comparisons. *Risk Analysis*, 2008; 4:1115–1124.
13. Coleman ME, Thran B, Morse SS, Hugh-Jones M, Massulik S. Inhalation anthrax: Dose response and risk analysis. *Biosecurity and Bioterrorism-Biodefense Strategy Practice and Science*, 2008; 2:147–159.
14. Kaufmann AF, Meltzer MI, Schmid GP. The economic impact of a bioterrorist attack: Are prevention and postattack intervention programs justifiable? *Emerging Infectious Diseases*, 1997; 2:83–94.
15. Cox LA. Some limitations of “risk = threat x vulnerability x consequence” for risk analysis of terrorist attacks. *Risk Analysis*, 2008; 6:1749–1761.
16. Cox LA, Popken DA. Overcoming confirmation bias in causal attribution: A case study of antibiotic resistance risks. *Risk Analysis*, 2008; 5:1155–1171.
17. Cox LA. Internal dose, uncertainty analysis, and complexity of risk models. *Environment International*, 1999; 6–7:841–852.
18. Huang Y, Hong T, Bartrand TA, Gurian PL, Haas CN, Liu R, Tamrakar SB. How sensitive is safe? Risk-based targets for ambient monitoring of pathogens. *Sensors Journal, IEEE*, 2010; 3:668–673.
19. Mitchell-Blackwood J, Gurian PL. Finding risk-based switchover points for response decisions for environmental exposure to *Bacillus anthracis* (in press). *Human and Ecological Risk Assessment*, 2010.
20. Sego L, Anderson K, Matzke B, Sieber K, Shulman S, Bennett J, Gillen M, Wilson J, Pulsipher B. An Environmental Sampling Model for Combining Judgment and Randomly Placed Samples. Richland, WA. Pacific Northwest National Laboratory, PNNL-16636, 2007.

21. Canter DA, Gunning D, Rodgers P, O'Connor L, Traunero C, Kemper CJ. Remediation of *Bacillus anthracis* contamination in the US Department of Justice mail facility. *Biosecurity and Bioterrorism-Biodefense Strategy Practice and Science*, 2005; 2:119–127.
22. Canter DA. Addressing residual risk issues at anthrax cleanups: How clean is safe? *Journal of Toxicology and Environmental Health, Part A: Current Issues*, 2005; 11:1017–1032.
23. Canter DA. Remediating anthrax-contaminated sites: Learning from the past to protect the future. *Chemical Health and Safety*, 2004; 4:13–19.
24. Brown GS, Betty RG, Brockmann JE, Lucero DA, Souza CA, Walsh KS, Boucher RM, Tezak M, Wilson MC, Rudolph T. Evaluation of a wipe surface sample method for collection of *Bacillus* spores from nonporous surfaces. *Applied and Environmental Microbiology*, 2007; 3:706–710.
25. Edmonds JM, Collett PJ, Valdes ER, Skowronski EW, Pelletier GJ, Emanuel PA. Surface sampling of spores in dry-deposition aerosols. *Applied and Environmental Microbiology*, 2009; 1:39–44.
26. Edmonds JM. Efficient methods for large-area surface sampling of sites contaminated with pathogenic microorganisms and other hazardous agents: Current state, needs, and perspectives. *Applied Microbiology and Biotechnology*, 2009; 5:811–816.
27. GAO. Capitol Hill Anthrax Incident: EPA's Cleanup Was Successful; Opportunities Exist to Enhance Contract Oversight. Washington, DC: GAO-03-686, 2003.
28. Sego LH, Wilson JE. Accounting for False Negatives in Hotspot Detection. Richland, WA. Pacific Northwest National Laboratory, PNNL-16812, 2007.
29. Jernigan JA, Stephens DS, Ashford DA, Omenaca C, Topiel MS, Galbraith M, Tapper M, Fisk TL, Zaki S, Popovic T, Meyer RF, Quinn CP, Harper SA, Fridkin SK, Sejvar JJ, Shepard CW, McConnell M, Guarner J, Shieh WJ, Malecki JM, Gerberding JL, Hughes JM, Perkins BA. Bioterrorism-related inhalational anthrax: The first 10 cases reported in the United States. *Emerging Infectious Diseases*, 2001; 6:933–944.
30. Holty JEC, Bravata DM, Liu H, Olshen RA, McDonald KM, Owens DK. Systematic review: A century of inhalational anthrax cases from 1900 to 2005. *Annals of Internal Medicine*, 2006; 4:270–280.
31. Whitfield WJ. A study of the effects of relative humidity on small particle adhesion to surfaces. Pp. 73–81 in Mittal KL (ed). *Surface Contamination: Genesis, Detection and Control*. New York: Plenum Press, 1979.
32. Whitfield WJ. A study of the effects of relative humidity on small particle adhesion to surfaces. Pp. 73–81 in Mittal KL (ed). *Surface Contamination: Genesis, Detection and Control*. New York: Plenum Press, 1979.
33. Mitchell-Blackwood J, Gurian PL, Weir M. A hierarchical model for probabilistic dose-response assessment of *Bacillus anthracis*. In *Proceedings of the Second Annual DHS University Network Summit*, Washington, DC, 2008.
34. Manchee RJ, Broster MG, Melling J, Henstridge RM, Stagg AJ. *Bacillus anthracis* on Gruinard Island. *Nature*, 1981; 5838:254–255.
35. Sinclair R, Boone SA, Greenberg D, Keim P, Gerba CP. Persistence of category a select agents in the environment. *Applied and Environmental Microbiology*, 2008; 3:555–563.
36. Haas CN, Rose JB, Gerba CP. *Quantitative Microbial Risk Assessment*. New York: Wiley, 1999.
37. Furumoto WA, Mickey R. A mathematical model for the infectivity-dilution curve of tobacco mosaic virus: Theoretical considerations. *Virology*, 1967; 2:216–223.
38. Furumoto WA, Mickey R. A mathematical model for the infectivity-dilution curve of tobacco mosaic virus: Experimental tests. *Virology*, 1967; 2:224–233.
39. Buchholz H. *The Confluent Hypergeometric Function*. New York: Springer, 1969.
40. Teunis PFM, Havelaar AH. The beta Poisson dose-response model is not a single-hit model. *Risk Analysis*, 2000; 4:513–520.
41. Thatcher TL, Layton DW. Deposition, resuspension, and penetration of particles within a residence. *Atmospheric Environment*, 1995; 13:1487–1497.
42. Herzog AB, McLennan SD, Pandey AK, Gerba CP, Haas CN, Rose JB, Hashsham SA. Implications of detection limit of various methods for *Bacillus anthracis* in computing risk to human health. *Applied and Environmental Microbiology*, 2009; 75:6331–6339.
43. Teunis PFM, Havelaar AH. Risk assessment for protozoan parasites. *International Biodeterioration & Biodegradation*, 2002; 3–4:185–193.
44. Wada K, Tanaka H, Suyama T, Kimura H, Yamamoto T. Numerical simulation of dust aggregate collisions. II. Compression and disruption of three-dimensional aggregates in head-on collisions. *Astrophysical Journal*, 2008; 2:1296–1308.
45. Elimelech M, Gregory J, Jia X, Williams RA. *Particle Deposition and Aggregation—Measurement, Modelling and Simulation*. Woburn, MA: Butterworth-Heinemann, 1995.
46. Blum J. *Dust Agglomeration*. *Advances in Physics*, 2006; 7–8:881–947.
47. Barnes JM. The removal of bacteria from glass surfaces with calcium alginate, gauze and absorbent cotton wool swabs. *Journal of Applied Microbiology*, 1952; 1:34–40.
48. Angelotti R, Foter MJ, Buschand KA, Lewis KH. A comparative evaluation of methods for determining the bacterial contamination of surfaces. *Journal of Food Science*, 1958; 2:175–185.
49. Sanderson WT, Hein MJ, Taylor L, Curwin BD, Kinnes GM, Seitz TA, Popovic T, Holmes HT, Kellum ME, McAllister SK, Whaley DN, Tupin EA, Walker T, Freed JA, Small DS, Klusaritz B, Bridges JH. Surface sampling methods for *Bacillus anthracis* spore contamination. *Emerging Infectious Diseases*, 2002; 10:1145–1151.
50. Rose L, Jensen B, Peterson A, Banerjee SN, Arduino MJ. Swab materials and *Bacillus anthracis* spore recovery from nonporous surfaces. *Emerging Infectious Diseases*, 2004; 6:1023–1029.
51. Frawley DA, Samaan MN, Bull RL, Robertson JM, Mateczun AJ, Turnbull PCB. Recovery efficiencies of anthrax spores and ricin from nonporous or nonabsorbent and porous or absorbent surfaces by a variety of sampling methods. *Journal of Forensic Sciences*, 2008; 5:1102–1107.
52. Estill CF, Baron PA, Beard JK, Hein MJ, Larsen LD, Rose L, Schaefer FW III, Noble-Wang J, Hodges L, Lindquist HDA, Deye GJ, Arduino MJ. Recovery efficiency and limit of detection of aerosolized *Bacillus anthracis* spores from environmental surface samples. *Applied and Environmental Microbiology*, 2009; 13:4297–4306.
53. Hong T. Estimating risk of exposure to *Bacillus anthracis* based on environmental concentration. Drexel, 2009. Available at: <http://idea.library.drexel.edu/bitstream/1860/3012/3/Hong%20Estimating%20Risk.pdf>.
54. EPA. *Exposure Factors Handbook*. Washington, DC: Exposure Assessment Group, Office of Health and Environmental Assessment, U.S. Environmental Protection Agency, 1997.
55. Kowalski WJ. *Immune Building System Technology*. New York: McGraw-Hill, 2003.
56. Clemen RT, Reilly T. *Making Hard Decisions*. Belmont, CA: Duxbury Press, 2001.
57. NRC. *Reopening Public Facilities After a Biological Attack: A Decision-Making Framework*. Washington, DC: National Academies Press, 2005.
58. Skolnick EB, Hamilton RG. Legacy science suggests improved surface-testing practices for detection of dispersed

- bioagents in bioterrorism response. In Proceedings of 2004 National Environmental Monitoring Conference, Washington, DC.
59. Hong T, Gurian PL. Key uncertainties in risk informed standards for *B. anthracis*. Pp. 252–257 in Proceedings of 2nd International Conference on Risk Analysis and Crisis Response, October 19–21, Beijing, 2009.
 60. Varga RS. Geršgorin and His Circles. Berlin: Springer-Verlag, 2004.
 61. Roman S. Advanced Linear Algebra. New York: Springer, 2008.
 62. Landahl H. On the removal of air-borne droplets by the human respiratory tract: I. Lung Bulletin of Mathematical Biology, 1950; 1:43–56.
 63. ASHRAE. ASHRAE Handbook. Atlanta: ASHRAE, 2005.
 64. Lai ACK, Nazaroff WW. Modeling indoor particle deposition from turbulent flow onto smooth surfaces. Journal of Aerosol Science, 2000; 4:463–476.
 65. Riley WJ, McKone TE, Lai ACK, Nazaroff WW. Indoor particulate matter of outdoor origin: Importance of size-dependent removal mechanisms. Environmental Science & Technology, 2002; 2:200–207.
 66. Schneider T, Kildeso J, Breum NO. A two compartment model for determining the contribution of sources, surface deposition and resuspension to air and surface dust concentration levels in occupied rooms. Building and Environment, 1999; 5:583–595.
 67. Schlesinger, RB. Deposition and clearance of inhaled particles. Pp. 191–217 in McClellan RO, Henderson RF (eds). Concepts in Inhalation Toxicology. Washington, DC: Taylor: Francis, 1989.
 68. Mitchell-Blackwood J, O'Donnell C, Gurian PL. An evaluation of the risk threshold for prophylaxis and treatment after an anthrax release. Society for Risk Analysis Annual Meeting, Boston, 2008.
 69. Travis CC, Richter SA, Crouch EAC, Wilson R, Klema ED. Cancer risk management. Environmental Science & Technology, 1987; 5:415–420.